

Optical Analogues for Massless Dirac Particles and Conical Diffraction in One Dimension

J. M. Zeuner,¹ N. K. Efremidis,² R. Keil,¹ F. Dreisow,¹ D. N. Christodoulides,³ A. Tünnermann,¹
S. Nolte,¹ and A. Szameit^{1,*}

¹*Institute of Applied Physics, Friedrich-Schiller-University Jena, Max-Wien-Platz 1, 07743 Jena, Germany*

²*Department of Applied Mathematics, University of Crete, GR-71409 Heraklion, Crete, Greece*

³*Center for Research and Education in Optics and Lasers, School of Optics, University of Central Florida,
Orlando, Florida 32816, USA*

(Received 23 February 2012; published 13 July 2012)

We demonstrate that light propagating in an appropriately designed lattice can exhibit dynamics akin to that expected from massless relativistic particles as governed by the one-dimensional Dirac equation. This is accomplished by employing a waveguide array with alternating positive and negative effective coupling coefficients, having a band structure with two intersecting minibands. Through this approach optical analogues of massless particle-antiparticle pairs are experimentally realized. One-dimensional conical diffraction is also observed for the first time in this work.

DOI: [10.1103/PhysRevLett.109.023602](https://doi.org/10.1103/PhysRevLett.109.023602)

PACS numbers: 42.50.Xa, 03.65.Pm, 42.82.Et

The Dirac wave equation, formulated in 1928 by Dirac [1], represents one of the great breakthroughs of theoretical physics. This equation unifies the principles of quantum mechanics and special relativity, suggesting in particular a new form of matter: antimatter, that predated its experimental discovery [2]. Importantly, the Dirac theory does not only describe massive particle-antiparticle pairs but also potentially massless fermions, such as neutrinos and anti-neutrinos [3]. However, direct experimental observation of such entities is highly intricate since such particles do only weakly interact with matter [4]. Classical optical emulators of the Dirac equation recently received a great deal of interest since, with their help, various relativistic phenomena can be experimentally observed in tabletop experiments [5–9]. In all of these demonstrations, a biatomic superlattice waveguide array was used to simulate the spinor-type wave function of the Dirac equation. However, this carries the intrinsic drawback that a band gap opens between the two minibands, which is physically equivalent to a mass in the emulated Dirac equation leading to the fact that only massive Dirac particles can be simulated. To date, the only known optical realization of a massless Dirac equation is in the two-dimensional (2D) setting of honeycomb photonic lattices [10,11] that consists of two shifted hexagonal lattices. Therefore, this structure represents a superlattice with identical waveguides and, hence, without a gap between the bands of eigenmodes. The honeycomb structure, which resembles the geometry of electronic graphene, can consequently be used for realizing optical simulations of the 2D versions of Klein tunneling [12] and *Zitterbewegung* [13]. It is usually believed that gapless superlattices exist only in settings with two transverse dimensions, and one-dimensional (1D) superlattices always exhibit an interband gap. However, 1D systems are particularly useful in isolating certain phenomena associated with

the Dirac equation that may be too intricate to generate in systems with higher dimensions.

As it is commonly known, the band structure of a massless Dirac equation features a particular conical intersection point between the two minibands—the Dirac point (also called “diabolic” point). These points, that were first described by Hamilton in the context of biaxial crystals [14], are characterized by their singularity; i.e., no uniquely defined group velocity exists at such points. Importantly, this gives rise to the peculiar phenomenon, amongst others, of conical diffraction [14], where a light beam, launched into a biaxial crystal at the direction of the diabolic points, spreads in a conical fashion. The light forms a thin ring with an increasing radius during propagation, but the thickness of the ring stays constant over the whole propagation distance. Following Hamilton’s prediction, conical diffraction was first experimentally observed by Lloyd [15] and is, therefore, the first theoretically predicted physical phenomenon ever. Interestingly, conical diffraction attracts attention until today [16–21]. Even though this concept was introduced in the field of crystal optics, it can be transferred to other fields of physics, where such diabolic points exist. This became particularly clear in the work of Peleg *et al.* [10], where conical diffraction was associated with the diabolic points in the honeycomb structure, although the physical origin is slightly different in that system. To date, diabolic points have never been realized in a 1D structure, and—consequently—conical diffraction has never been observed in a 1D geometry.

In our work, we present the first experimental implementation of the 1D massless Dirac equation that exhibits a conical intersection in the band structure. We demonstrate the optical analogue to a massless relativistic particle and its antiparticle moving away from each other. Additionally, we draw a connection from this phenomenon to 1D conical diffraction, a surprising result that emphasizes the close

analogy between conical diffraction and the evolution of massless Dirac particles. In order to implement a conical intersection in a 1D system, we show that the Dirac equation in its discretized form can be mapped on a lattice with alternating positive and negative coupling, a setting that was theoretically introduced only recently [22]. Note, that our setting provides a superlattice with two identical sites per unit cell, preventing the opening of a gap between the bands and facilitating the formation of a conical intersection point. This is in contrast to all 1D settings that were realized before, in which the superlattices were implemented by alternating refractive indices of adjacent waveguides opening a photonic gap between two minibands of eigenmodes.

To theoretically introduce our ideas, we assume a waveguide array that consists of single-mode waveguides sinusoidally curved along the propagation direction z with the transverse position of the waveguide centers $\xi_0(z) = A \cos(\frac{2\pi}{P}z)$, where A is the modulation amplitude, and P is the period. A sketch of the setup is shown in Fig. 1(a). The propagation of light in such weakly coupled waveguides with nearest-neighbor interaction is described by the tight-binding model [23]:

$$i\partial_z \phi_j + c_j \phi_{j-1} + c_{j+1} \phi_{j+1} + \ddot{\xi}_0(z) x_j \frac{2\pi n_0}{\lambda} \phi_j = 0, \quad (1)$$

where ϕ_j is the amplitude of the optical wave in the j th waveguide, x_j is the waveguide position, n_0 is the

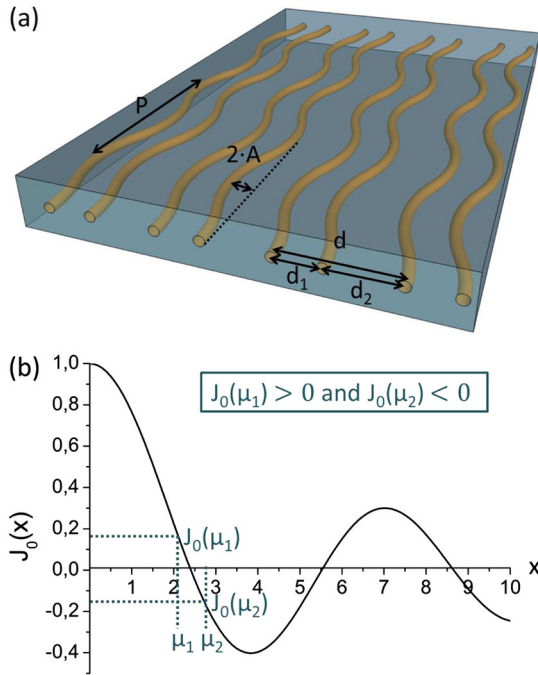


FIG. 1 (color online). (a) Scheme of the waveguide setup. (b) Zero-order Bessel function with two marked values needed for the calculation of the special effective coupling modulation.

refractive index of the bulk, and c_j is the coupling constant between the j th and $(j-1)$ th guide in a straight array with $\xi_0 \equiv 0$ for a certain distance $x_j - x_{j-1}$. The superlattice geometry is introduced by an alternating change of the spacing between the identical sites. The effective coupling coefficient after every period of the sinusoidally curved waveguides can be computed using averaging methods and is given by [23]

$$c_{\text{eff}} = c_j J_0 \left(A \frac{4\pi^2 n_0}{P\lambda} (x_j - x_{j-1}) \right), \quad (2)$$

where J_0 is the lowest-order Bessel function of the first kind. By varying the distance between adjacent guides, the effective coupling constant changes. If we assume that ν_1 and ν_2 are two subsequent roots of the Bessel function, we can find values $\mu_1 < \nu_1 < \mu_2 < \nu_2$, so that $J_0(\mu_1)$ has a positive sign and $J_0(\mu_2)$ a negative sign [for explanation see also Fig. 1(b)]. Hence, for certain values of the spacing between adjacent lattice sites d_1 and d_2 , we can meet the following requirements:

$$c_{\text{eff}} = c(d_1)J_0(\mu_1(d_1)) \quad - \quad c_{\text{eff}} = c(d_2)J_0(\mu_2(d_2)).$$

Therefore, we are able to create a superlattice with alternating positive and negative effective coupling by an alternation of the distances between adjacent guides. Importantly, the refractive indices of all sites are identical. The resulting effective coupled mode equations read

$$i\partial_z \phi_j + c_{\text{eff}}(-1)^j (\phi_{j-1} - \phi_{j+1}) = 0. \quad (3)$$

Equation (3) was introduced in [22]; however, our implementation is different from the one suggested in that work, where the alternating coupling was achieved by a longitudinal modulation of the refractive index of the waveguides.

Interestingly, a 1D lattice with alternating positive and negative coupling can be transformed to a 1D Dirac equation of a massless relativistic particle. If the lattice described in Eq. (3) is divided into two sublattices with propagating amplitudes a_j and b_j , the coupled mode equations

$$i\partial_z a_j - c_{\text{eff}}(b_j - b_{j-1}) = 0 \quad (4)$$

$$i\partial_z b_j - c_{\text{eff}}(a_j - a_{j+1}) = 0 \quad (5)$$

can be rewritten as

$$i\partial_z A_j + ic_{\text{eff}}(B_j - B_{j-1}) = 0 \quad (6)$$

$$i\partial_z B_j + ic_{\text{eff}}(A_{j+1} - A_j) = 0, \quad (7)$$

using the substitutions $a_j = A_j$ and $b_j = -iB_j$. With the definition of the discrete derivative $\partial_x A \rightarrow A_{j+1} - A_j$ and $\partial_x B \rightarrow B_j - B_{j-1}$, the two-component spinor $\Psi = (A, B)^T$, and the Pauli matrix σ_x , one finally arrives at a *discretized* 1D Dirac equation for a massless particle:

$$i\partial_z \Psi + ic_{\text{eff}} \sigma_x \partial_x \Psi = 0, \quad (8)$$

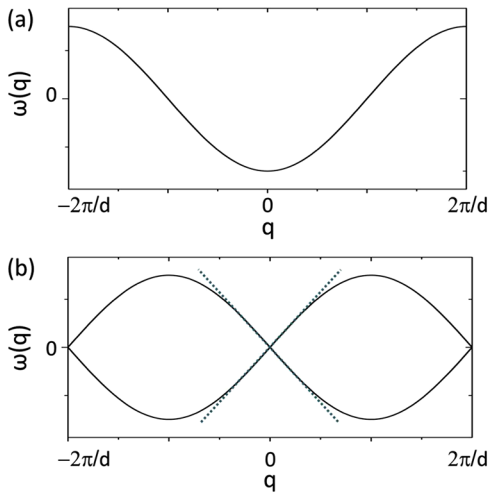


FIG. 2 (color online). (a) Dispersion relation of a straight lattice with equal spacing. (b) Dispersion relation of the lattice demonstrated here, which shows an intersection of the two minibands and a linear slope (marked by the dotted lines) in the center of the first Brillouin zone.

where c_{eff} as the effective coupling constant is the analogue of the speed of light. Due to the equivalence of Eq. (3) and the 1D Dirac equation [Eq. (8)], the spatial propagation of a monochromatic light field in our waveguide lattice directly simulates the temporal evolution of a massless relativistic particle in one spatial dimension. This analogy also manifests in reciprocal space, in the band structure of the system. In a regular array with constant spacing, the relation between the longitudinal wave number ω and the transversal wave number q reads $\omega = -2c \cos(q \frac{d}{2})$, with d as the spacing between next-nearest sites and is shown in Fig. 2(a). In contrast, for our superlattice structure the dispersion relation reads $\omega = \pm 2c \sin(q \frac{d}{2})$. This can be calculated directly from the coupled mode equations [Eq. (3)] by making a plane wave ansatz $\phi_j(q) \sim \exp(iqj \frac{d}{2} - i\omega z)$. A graphic presentation of the band structure is shown in Fig. 2(b). Two minibands are formed, which intersect at $q = 0$. Importantly, in the vicinity of this intersection point, the minibands have a slope that is approximately linear, as a Taylor expansion of the dispersion relation shows. Hence,

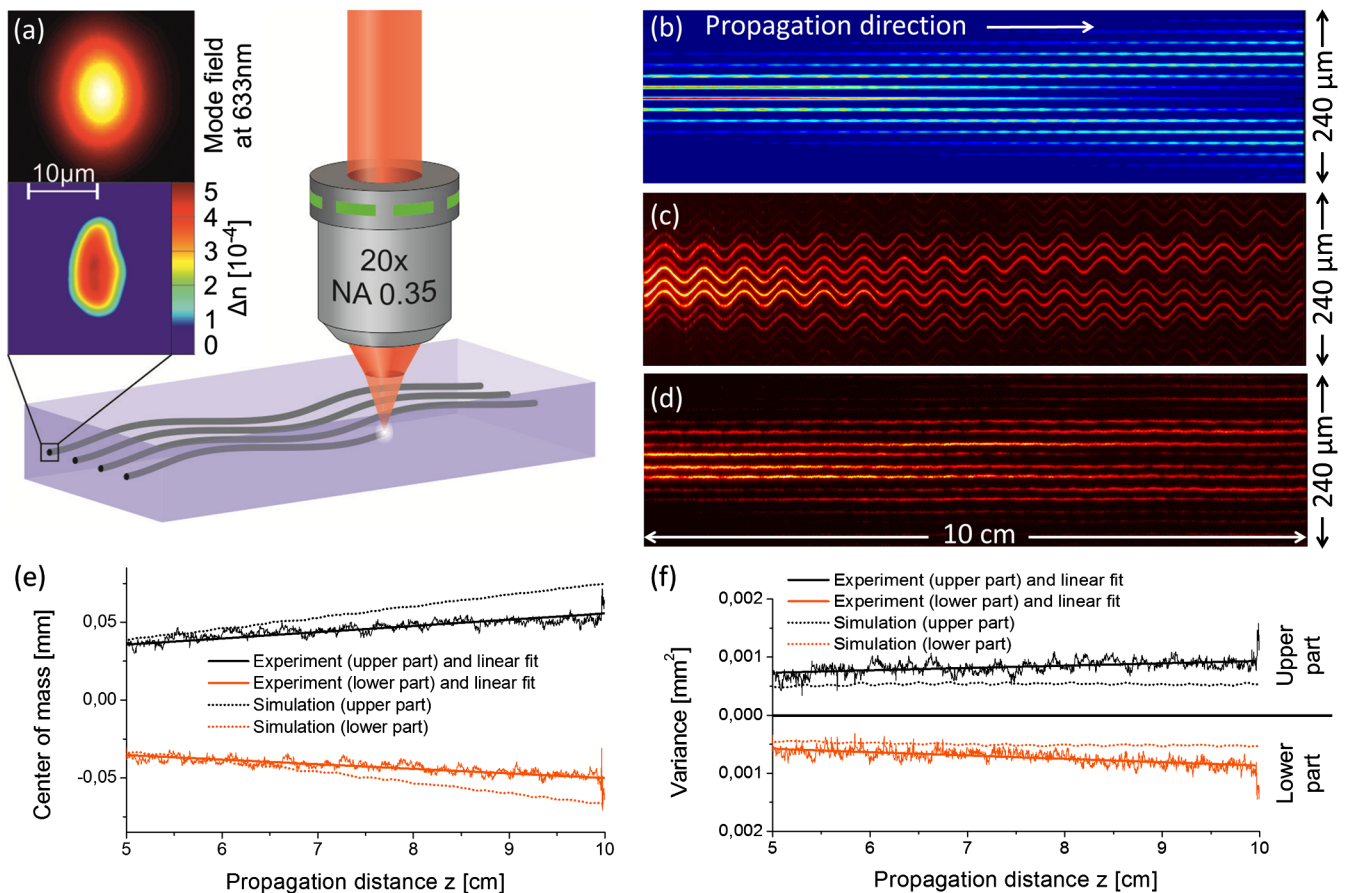


FIG. 3 (color online). (a) Fabrication of the waveguides by laser writing process, cross section of the resulting mode field, and refractive index profile. (b) Simulation of the light propagation. Parameters are given in the text. (c) Experimental fluorescence image, at which in (d) the sinusoidal waveguide structure was digitally straightened and losses were removed. (e) Center of mass and (f) variance of upper and lower part of (d).

this intersection point resembles a Dirac or diabolic point that was described above. If an initial beam is perpendicularly ($q_0 = 0$) launched into such a waveguide array, the wave splits into two equal parts that propagate with opposite group velocities (defined by the 1st derivative of the dispersion relation) and zero diffraction (defined by the 2nd derivative). This is exactly what conical diffraction means. Note that due to this exceptional point, there is no gap between the minibands.

For our experiments, we fabricated a waveguide array by employing the femtosecond direct-writing approach [24] as shown in Fig. 3(a). The parameters of the writing procedure can be found in [24]. The sample consists of 40 sinusoidally shaped waveguides with alternating distances between adjacent lattice sites equal to $d_1 = 13.9 \mu\text{m}$ and $d_2 = 18.1 \mu\text{m}$, that are written into a 10 cm long fused silica wafer. The curvature of the guides has a period of $P = 6 \text{ mm}$, and the amplitude is $A = 10.1 \mu\text{m}$. These parameters yield effective coupling coefficients of $c_{\text{eff}} \approx \pm 0.2 \text{ cm}^{-1}$. A sketch of the setup is shown in Fig. 1(a).

For visualizing the light propagation, we employ a fluorescence microscopy technique [25]. We launch a broad Gaussian beam with a wavelength of 633 nm, covering about 5 waveguides, straight into the array. The light used for the excitation was linearly polarized in a direction perpendicular to the lattice plane. A simulation and the associated experimentally obtained fluorescence image are shown in Figs. 3(b) and 3(c). In Fig. 3(d), the sinusoidal shape and the losses of the waveguides were digitally removed for a better comparison of the experimental image with the simulated image. The splitting of the ray bundle into two nonspreading parts moving away from each other in a constant fashion is clearly seen. To confirm this observation, we computed the center of mass [Fig. 3(e)] and the variance [Fig. 3(f)] of the upper and lower half of Fig. 3(d). The centers of mass of both beams move away from each other, in a linear fashion, as shown in Fig. 3(e). Additionally, the variance of both beams, plotted in Fig. 3(f), stays nearly constant during propagation. These effects are characteristic for the phenomenon of conical diffraction and is based on the linear slope of the band structure [marked by the dotted line in Fig. 2(b)] in the vicinity of the singularity. In contrast to our simulations, there is a very slight broadening of both beams visible in the experiment. The minor discrepancies in Figs. 3(e) and 3(f) between experimental and theoretical data are due to higher order coupling, which is not contained in the tight-binding approach in Eq. (1), and due to small inaccuracies occurring during the writing process that result in slightly different values for the coupling constant in experiment and simulation. However, the broadening of both beams is still much weaker than that of a Gaussian excitation in a lattice with similar spacing but only positive coupling coefficients, where the spreading is 10 times stronger than in our setting.

The splitting of the initial wave packet into two separate beams can also be interpreted in terms of relativistic quan-

tum mechanics, based on the Dirac equation. The two counterpropagating beams in Figs. 3(b)–3(d) represent an optical analogue to two massless fermions (a particle and the corresponding antiparticle, e.g., a neutrino-antineutrino pair) moving away from each other. In the quantum mechanical analogue, the relativistic momentum of a particle reads $p = \pm((V - E)^2 - m^2c^4)^{1/2}/c$, which simplifies in the massless case without potential ($m = 0$, $V = 0$) to $p = \pm E/c$.

In conclusion, we demonstrated the optical emulation of the evolution of 1D massless Dirac fermions. We furthermore provided the first experimental proof of 1D conical diffraction. Our results yield surprising evidence for the close relationship between the two seemingly unconnected phenomena of 1D conical diffraction and the evolution of massless Dirac particles. In order to experimentally implement our results, we mapped the discretized version of the 1D Dirac equation to a lattice with alternating positive and negative coupling between adjacent sites and realized this setting using periodically curved waveguides in a position-based superlattice. Our work is a leap into the emulation of 1D relativistic phenomena of massless particles on a lattice, a concept which is not restricted to waveguide arrays but is also applicable to other systems like ultracold quantum gases and trapped ions [26]. As the interaction among particles in many-body systems in a mean-field approximation can be described by a nonlinear term in the evolution equation, we envision on our platform further optical experiments employing nonlinearity that will allow the emulation of relativistic interacting particles [27].

The authors wish to thank the German Ministry of Education and Research (Center for Innovation Competence program, Grant No. 03Z1HN31). N. K. E. is supported by an ‘‘ARISTEIA’’ Action of the ‘‘OPERATIONAL PROGRAMME EDUCATION AND LIFELONG LEARNING’’ that is co-funded by the European Social Fund (ESF) and National Resources.

*alexander.szameit@uni-jena.de

- [1] P. A. M. Dirac, *Proc. R. Soc. A* **117**, 610 (1928).
- [2] C. D. Anderson, *Phys. Rev.* **43**, 491 (1933).
- [3] E. Fermi, *Z. Phys.* **88**, 161 (1934).
- [4] C. L. Cowan, F. Reines, F. B. Harrison, H. W. Kruse, and A. D. McGuire, *Science* **124**, 103 (1956).
- [5] F. Dreisow, M. Heinrich, R. Keil, A. Tünnermann, S. Nolte, S. Longhi, and A. Szameit, *Phys. Rev. Lett.* **105**, 143902 (2010).
- [6] S. Longhi, *Opt. Lett.* **35**, 235 (2010).
- [7] F. Dreisow, R. Keil, A. Tünnermann, S. Nolte, S. Longhi, and A. Szameit, *Europhys. Lett.* **97**, 10008 (2012).
- [8] S. Longhi, *Phys. Rev. B* **81**, 075102 (2010).
- [9] S. Longhi, *Phys. Rev. A* **81**, 022118 (2010).
- [10] O. Peleg, G. Bartal, B. Freedman, O. Manela, M. Segev, and D. N. Christodoulides, *Phys. Rev. Lett.* **98**, 103901 (2007).

- [11] A. Szameit, M. C. Rechtsman, O. Bahat-Treidel, and M. Segev, *Phys. Rev. A* **84**, 021806 (2011).
- [12] O. Bahat-Treidel, O. Peleg, M. Grobman, N. Shapira, M. Segev, and T. Pereg-Barnea, *Phys. Rev. Lett.* **104**, 063901 (2010).
- [13] X. Zhang, *Phys. Rev. Lett.* **100**, 113903 (2008).
- [14] W. Hamilton, *Trans. R. Irish Acad.* **17**, 1 (1837), <http://www.jstor.org/stable/30078785>.
- [15] H. Lloyd, *Trans. R. Irish Acad.* **17**, 145 (1837), <http://www.jstor.org/stable/30078786>.
- [16] R. Potter, *Philos. Mag.* **18**, 343 (1841).
- [17] C. V. Raman, V. S. Rajagopalan, and T. M. K. Nedungadi, *Proc. Mat. Sci.* **14**, 221 (1941), <http://www.springerlink.com/content/4711652777642416/>.
- [18] A. J. Schell and N. Bloembergen, *J. Opt. Soc. Am.* **68**, 1093 (1978).
- [19] J. Feve, B. Boulanger, and G. Marnier, *Opt. Commun.* **105**, 243 (1994).
- [20] A. Belsky and M. Stepanov, *Opt. Commun.* **204**, 1 (2002).
- [21] M. Berry and M. Jeffrey, in *Progress in Optics* (Elsevier, New York, 2007), Vol. 50, p. 1350.
- [22] N. K. Efremidis, P. Zhang, Z. Chen, D. N. Christodoulides, C. E. Rüter, and D. Kip, *Phys. Rev. A* **81**, 053817 (2010).
- [23] S. Longhi, M. Marangoni, M. Lobino, R. Ramponi, P. Laporta, E. Cianci, and V. Foglietti, *Phys. Rev. Lett.* **96**, 243901 (2006).
- [24] A. Szameit and S. Nolte, *J. Phys. B* **43**, 163001 (2010).
- [25] A. Szameit, F. Dreisow, H. Hartung, S. Nolte, A. Tünnermann, and F. Lederer, *Appl. Phys. Lett.* **90**, 241113 (2007).
- [26] I. Bloch, J. Dalibard, and W. Zwerger, *Rev. Mod. Phys.* **80**, 885 (2008).
- [27] Y. Lahini, M. Verbin, S. D. Huber, Y. Bromberg, R. Pugatch, and Y. Silberberg, <http://arxiv.org/abs/1105.2273v1>.